^{13}C Solid-state NMR Study on Populations, Conformations, and Molecular Motions of γ-Valerolactone Enantiomers Enclathrated in the Chiral Cholic acid Host

Fumio Imashiro,* Daisuke Kuwahara and Takehiko Terao*
Department of Chemistry, Faculty of Science, Kyoto University, Kyoto 606-01, Japan

^{13}C Solid-state NMR spectra were measured for γ-valerolactone in the cholic-acid host which exhibits efficient optical resolution. Both the more-favoured (*S*)-(−)-enantiomer [(*S*)-**1**] and the less-favoured (*R*)-(+)-enantiomer [(*R*)-**1**] of γ-valerolactone were found to coexist microscopically in the cholic-acid channels by two-dimensional exchange NMR. Their populations were non-destructively determined from the intensities of their methyl-carbon signals. The principal values of the ^{13}C chemical-shift tensors for the methyl carbons were determined by the one-dimensional switching-angle sample spinning (1D-SASS) NMR method. By comparing the ^{13}C chemical-shift tensors with those calculated by the *ab initio* GIAO method, the conformation of each enantiomer was determined as follows: (*S*)-**1** has the methyl group in the equatorial direction to the five-membered ring of γ-valerolactone, while (*R*)-**1** has it in the axial direction. The optical resolution of γ-valerolactone by the inclusion method using the cholic-acid host is mainly ascribed to the energy difference in the conformations of γ-valerolactone. Temperature variation of the ^{13}C chemical-shift powder pattern for the methyl carbons of both enantiomers revealed the presence of an overall reorientation among a finite number of isotropically distributed sites accompanying slow rotational diffusion. The rate of the reorientation for (*S*)-**1** is higher than that for (*R*)-**1**; moreover, the corresponding barrier for (*S*)-**1** is notably lower than that for (*R*)-**1**.

Since 1987, interesting inclusion phenomena with a host of a steroidal bile acid, cholic acid (CA) have been reported by Miyata *et al.*[1-3] One of the significant features is that the cholic acid inclusion compounds (CAICs) can be prepared not only by recrystallization of CA from liquid guests but also by its absorption into unsolvated CA crystals. Another feature is efficient optical resolution of chiral guest molecules by enclathration into the CA channels.[2] The optical resolution of racemic γ-valerolactone (**1**) by recrystallization or absorption yields (*S*)-(−)-**1** [abbreviated hereafter as (*S*)-**1**, and the other enantiomer (*R*)-(+)-**1** as (*R*)-**1**] in 28 or 38% enantiomeric excess (e.e.), respectively,[2] which were determined by ^{1}H solution-state NMR spectroscopy using the chiral shift reagent, (*R*)-(−)-2,2,2-trifluoro-1-(9-anthryl)ethanol.

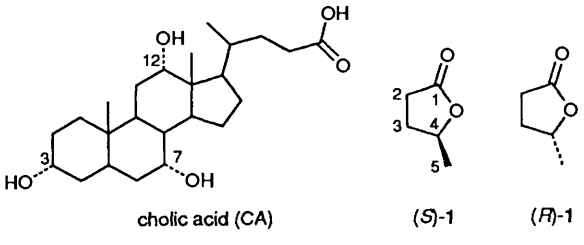

cholic acid (CA) (*S*)-**1** (*R*)-**1**

An X-ray diffraction study of CAIC prepared by recrystallization of CA from racemic **1** has recently been reported by Miki *et al.*[3] This study concluded that only the (*S*)-**1** molecules were included as the guest molecules in CAIC. This conclusion seems to be incompatible with the previous optical-resolution experiment. If we assume that both results are correct, two different CAIC crystals must exist, one of which includes only (*S*)-**1**, and the other only (*R*)-**1**, and the former crystal must have happened to be subjected to the X-ray diffraction experiment.

In the present study, we have investigated the state and behaviour of the guest molecules in CAIC by ^{13}C solid-state NMR spectroscopy. We prepared four different cholic acid/γ-valerolactone inclusion compounds (**I**–**IV**): **I** was obtained by recrystallization of CA from racemic **1**, whereas **II** was prepared by recrystallization of CA from **1** extracted from **I**. Absorption of nearly 100% e.e. (*S*)-**1** or racemic [5-^{13}C]**1** in CA yielded **III** or **IV**, respectively. We measured ^{13}C spectra by CPMAS and MAS for **I**–**IV**, two-dimensional (2D) exchange NMR for **IV**, and one-dimensional switching-angle sample spinning (1D-SASS) NMR[4] for **III** and **IV** in order to determine populations, conformations, and motions of the enantiomers of **1** in CAIC. We calculated the ^{13}C chemical-shift tensors for **1** by the coupled Hartree–Fock method with the gauge-invariant atomic orbitals (the *ab initio* GIAO method)[5] in order to confirm the conformations of the enantiomers by comparison with the experimental tensors.

Experimental

Materials.—[5-^{13}C]γ-Valerolactone ([5-^{13}C]-**1**) was prepared as follows: [^{13}C]methylmagnesium iodide was prepared from [99%-^{13}C]methyl iodide (5 g) and magnesium (0.85 g) in dry diethyl ether. The solvent was removed by distillation, and dry tetrahydrofuran (THF) was added. This Grignard reagent was added to a THF solution of ethyl succinyl chloride (5.76 g) and tris(acetylacetonate)iron(III) (0.38 g) as described in ref. 6. Ethyl [5-^{13}C]levulinate (2.1 g) thus obtained was subjected to reductive cyclization with sodium cyanoborohydride in THF at pH 2[7] to give 0.9 g of [5-^{13}C]-**1**.

Commercially available CA was recrystallized from methanol and dried under vacuum at 100 °C for 24 h. Recrystallization of CA (2 g) from commercially available racemic **1** (8 g) yielded **I** (2.3 g), whereas **II** (1.0 g) was prepared by recrystallization of CA (1 g) from **1** (3.2 g) extracted by direct distillation of **I** under vacuum. Nearly 100% e.e. (*S*)-**1** was obtained by five-times repeating absorption and distillation of **1**.[2] **III** And **IV** were obtained by absorption of the nearly 100% e.e. (*S*)-**1** and racemic [5-^{13}C]-**1**, respectively. All of the CAICs were washed with hexane and propyl ether to remove unincluded **1**. The

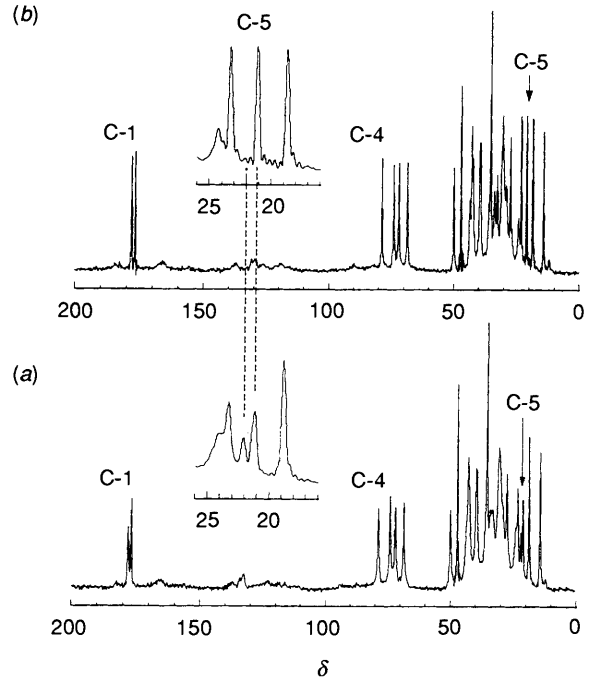

Fig. 1 ^{13}C CPMAS NMR Spectra of the cholic acid/γ-valerolactone inclusion compounds (**I** and **III**) at room temp. (*a*) **I**; (*b*) **III**. The resonance lines due to γ-valerolactone (**1**) are marked with their carbon numbers.

Table 1 Fractional populations *p* of the (*S*)-(−)-enantiomer [(*S*)-**1**] and (*R*)-(+)-enantiomer [(*R*)-**1**] of γ-valerolactone in the cholic-acid inclusion compounds **I**, **II** and **IV**

	^{13}C, solid[a]		^{1}H, soln[b]	
	(*S*)-**1** *p*/%	(*R*)-**1** *p*/%	(*S*)-**1** *p*/%	(*R*)-**1** *p*/%
I	64 ± 3	36 ± 3	66 ± 3	34 ± 3
II	81 ± 2	19 ± 2	78 ± 4	22 ± 4
IV	63 ± 2	37 ± 2		

[a] Determined from the ^{13}C solid-state MAS NMR spectra. [b] Determined from the ^{1}H solution-state NMR spectra with a chiral shift reagent, (*R*)-(−)-2,2,2-trifluoro-1-(9-anthryl)ethanol.

molar ratios of the host to guest components for all of the CAICs thus prepared were 1 : 1 within the experimental error of the elemental analysis.

NMR Measurements.—^{13}C Solid-state NMR spectra were measured by a modified JEOL GSX-200 spectrometer with a laboratory-built probe operating at 50.2 MHz. ^{13}C CPMAS Spectra were obtained with a cross-polarization time of 2 ms, a repetition time of 5 s, and a sample-spinning rate of 2.3 kHz, whereas ^{13}C MAS spectra (without cross-polarization) were measured with a repetition time of 30 s. The 2D exchange NMR spectra were obtained with a cross-polarization time of 2 ms, a repetition time of 4 s, and t_1 increments of 1 ms for 50 points. Variable-temperature 1D-SASS experiments were performed in the manner reported elsewhere[8] with an off-angle θ_{off} between 68.3 and 69.5°, a sample-spinning rate of 2.3 kHz, and a cross-polarization time of 2 ms.

Room-temperature ^{1}H solution-state NMR spectra were measured on a JEOL GX-400 spectrometer operating at 400 MHz.

Calculations.—Optimized geometries for stable conformers of **1** were obtained by both MM2 molecular mechanics calculations[9] and *ab initio* closed-shell Hartree–Fock calculations with the 4-31G basis set. The ^{13}C chemical-shift tensors for carbons of **1** in the isolated state were calculated by the coupled Hartree–Fock method with the 4-31G GIAOs. All of the molecular orbital calculations were performed with the *ab initio* calculation program KOTO[10] on a SONY NEWS-3260.

^{13}C Chemical-shift powder patterns reflecting molecular motions were obtained by the Abragam–Spiess' method[11] of calculating the correlation function of a spin system and the method based on a general density matrix formalism[12] by Alexander *et al.*[13]

Results and Discussion

Populations and Distribution of the Enantiomers.—The ^{13}C CPMAS NMR spectra for **I** and **III** are shown in Fig. 1, in which the resonance lines attributed to the C-1-carboxyl, C-4-etheral, and C-5-methyl carbons of **1** can be seen apart from CA lines. Those of the C-2- and C-3-methylene carbons of **1** cannot be identified because they are obscured by many host signals. The chemical shifts of the host signals are essentially identical for **I** and **III**, and the identifiable lines for CA show singlet lines in both **I** and **III**, indicating that the host channels consist of the same, sole CA species. The resonance lines of the C-1 and C-4 carbons of **1** in **I** and **III** appear as singlets at 178.0 and 78.8 ppm, respectively, from tetramethylsilane (TMS), whereas the C-5 carbon shows two lines at 21.1 and 22.0 ppm with different intensities for **I** [Fig. 1(*a*)], but a singlet at 21.1 ppm for **III** [Fig. 1(*b*)]. The ^{13}C CPMAS spectrum for **II** (not shown) is similar to that for **I** except that the upfield and downfield signals of the C-5 carbons are stronger and weaker, respectively, than those for **I**. The inclusion compound **III** involves only the (*S*)-**1** molecules, and **II** enclathrates them at a higher rate than **I**: therefore, we can assign the upfield C-5 resonance line in **I** and **II** to the C-5 carbon of (*S*)-**1** and the downfield one to that of (*R*)-**1**. The line-splitting for the C-5 carbon suggests that the two enantiomers have fixed and distinct conformations; the details will be discussed later.

Fractional populations of the two enantiomers of **1** in CAIC can non-destructively be determined from the lineshape analysis of the C-5 signals in the ^{13}C MAS spectra. On the other hand, they can also be evaluated from the lineshape analysis of the methyl signals in the ^{1}H solution-state NMR spectrum of **1** distilled from CAIC with (*R*)-(−)-2,2,2-trifluoro-1-(9-anthryl)-ethanol, which shifts the methyl proton signal of (*S*)-**1** more upfield than that of (*R*)-**1**.[14] The fractional populations evaluated in both ways for **I** and **II** are listed in Table 1, and agree with each other within the experimental error. The fractional populations of (*S*)-**1** and (*R*)-**1** in **IV** as evaluated from the ^{13}C MAS spectrum are in accord with those in **I** within the experimental error: no significant difference in the populations between the two preparation methods of CAIC was found.

Fig. 2(*a*) shows a 2D exchange NMR spectrum[15] measured for **IV** at 26.3 °C with a mixing time of 1.5 s, where the cross peaks between the two C-5 signals are clearly observed. In general, cross peaks in a 2D exchange spectrum originate from spin diffusion and/or chemical exchange. The latter may take place by conformational exchange in the present case. If this is the case, the cross peak intensities should increase at higher temperatures; however, no apparent changes were observed for the 2D exchange spectrum measured at 41.3 °C. We further observed the 2D exchange spectrum, applying a ^{1}H decoupling field of 6 G during the mixing time; then, the intensity of the cross peaks reduce substantially as shown in Fig. 2(*b*). These two experiments indicate that the observed cross peaks are attributed to spin diffusion. The residual cross peaks in the 2D spectrum with ^{1}H decoupling are caused by spin diffusion

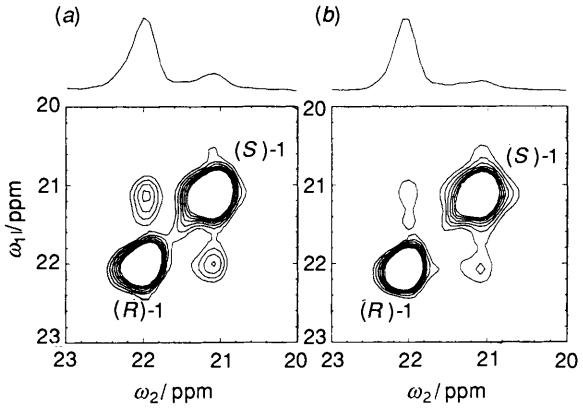

Fig. 2 ^{13}C 2D Exchange NMR spectra for the cholic acid/[5-^{13}C]γ-valerolactone (**1**) inclusion compound (**IV**) at 26.3 °C with a mixing time of 1.5 s. (*S*)-**1** and (*R*)-**1** represent the diagonal peaks of the C-5 carbons of the corresponding enantiomers of **1**. The upper spectra are cross sections at ω_1 = 22.0 ppm: (*a*) without decoupling during the mixing time; (*b*) with decoupling (6 G) during the mixing time.

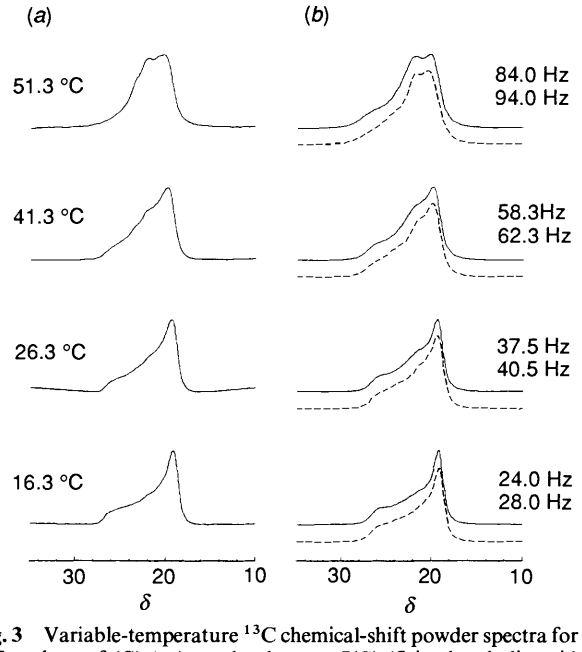

Fig. 3 Variable-temperature ^{13}C chemical-shift powder spectra for the C-5 carbon of (*S*)-(−)-γ-valerolactone [(*S*)-**1**] in the cholic acid/[5-^{13}C]γ-valerolactone inclusion compound (**IV**) with angles θ_{off} between 68.3 and 69.5°; therefore, each spectrum is scaled by a factor $P_2(\cos\theta_{off})$: (*a*) experimental spectra; (*b*) simulated spectra. Solid lines represent those for the reorientation among the octahedral sites with the rotational diffusion at the rate of 2.3, 1.7, 1.8 and 1.3 Hz with increasing temperatures. Broken lines represent those for the reorientation among the tetrahedral sites with the same rotational diffusion as above. The upper and the lower rate constants written in the Fig. stand for those of the former and the latter reorientations, respectively.

which is not perfectly quenched because the decoupling field has to be weak for the long-time irradiation. The occurrence of spin diffusion between the two enantiomers means that the (*S*)-**1** and (*R*)-**1** molecules are microscopically mixed in CAIC. Our conclusion negates the result by the X-ray crystallographic study that only (*S*)-**1** is involved in a crystal of CAIC.

Conformations of the Enantiomers.—The ^{13}C powder patterns for the C-5 carbons of (*S*)-**1** and (*R*)-**1** in **III** were separately observed by the 1D-SASS NMR method. Their spectra are dependent on temperature as illustrated in Figs. 3(*a*) and 4(*a*), respectively, from which molecular motions of the enantiomers will be clarified later. Here, we are concerned with only the ^{13}C chemical-shift parameters determined from the powder patterns obtained at the lowest temperature, which are

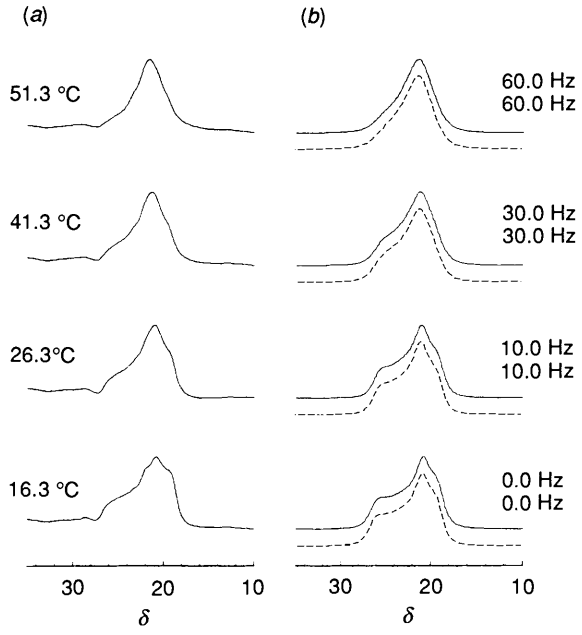

Fig. 4 Variable-temperature ^{13}C chemical-shift powder spectra for the C-5 carbon of (*R*)-(−)-γ-valerolactone [(*R*)-**1**] in the cholic acid/[5-^{13}C]γ-valerolactone inclusion compound (**IV**) with angles θ_{off} between 68.3 and 69.5°; therefore, each spectrum is scaled by a factor $P_2(\cos\theta_{off})$: (*a*) experimental spectra; (*b*) simulated spectra. Solid lines represent those for the reorientation among the octahedral sites with the rotational diffusion at the rate of 3.1, 3.0, 4.5 and 4.5 Hz with increasing temperatures. Broken lines represent those for the reorientation among the tetrahedral sites with the same rotational diffusion as above. The upper and the lower rate constants written in the Fig. stand for those of the former and the latter reorientations, respectively.

for almost stationary molecules. The anisotropy ($\Delta\sigma$) and the asymmetry patameter (η) of the ^{13}C chemical-shift tensors[16] were determined to be $\Delta\sigma = -18.7$ ppm and $\eta = 0.00$ for (*S*)-**1** and $\Delta\sigma = -17.5$ ppm and $\eta = 0.50$ for (*R*)-**1**. Although the $\Delta\sigma$ values are similar to each other, a substantial difference is found for the η values. This fact, as well as the isotropic shift difference, shows the presence of a conformational difference between the two enantiomers in CAIC, because the enantiomers with the same conformation should have the same chemical-shift tensor.

There are two stable conformers for **1** in the isolated state, one of which has the 5-methyl group in the equatorial position to the five-membered ring, and the other in the axial position as illustrated for both enantiomers in Fig. 5. The optimized geometries of the two conformers were obtained by MM2 molecular mechanics calculations as well as *ab initio* molecular orbital (MO) calculations; both results are in good agreement. The equatorial conformer was found to be more stable than the axial one by 0.46 and 0.48 kcal mol^{-1} by MM2 and *ab initio* MO calculations, respectively, and the potential barrier to the conformational exchange was estimated to be 1.40 kcal mol^{-1} by MM2 calculations. On the basis of the *ab initio* MO-optimized conformations the ^{13}C chemical-shift tensors were calculated by the *ab initio* GIAO method; the results are collected in Table 2. Although the σ_{iso} and $\Delta\sigma$ values calculated for the C-1, C-4 and C-5 carbons of the equatorial conformer are close to the corresponding values of the axial one, the η values for the C-5 carbons of the two conformers are different from each other; this situation is similar to the experimental case. Comparing the experimental and calculated η values for the C-5 carbons, we can conclude that the conformation of (*S*)-**1** is equatorial, whereas that of (*R*)-**1** is axial.

Using the 1D-SASS NMR method we also measured the ^{13}C powder patterns for the C-4 and C-5 carbons of (*S*)-**1** in **III**.

Table 2 Isotropic values σ_{iso}, anisotropies $\Delta\sigma$, and asymmetry parameters η of the ^{13}C chemical-shift tensors for the equatorial and axial conformers of γ-valerolactone (**1**) calculated by the *ab initio* GIAO method[a]

	Equatorial			Axial		
	σ_{iso}/ppm	$\Delta\sigma$/ppm	η	σ_{iso}/ppm	$\Delta\sigma$/ppm	η
C-1	19.45	−116.47	0.148	19.24	−116.12	0.122
C-2	177.87	23.37	0.854	180.38	24.39	0.647
C-3	178.71	23.21	0.956	181.22	−22.61	0.808
C-4	137.64	46.22	0.658	138.15	48.28	0.417
C-5	186.27	19.71	0.221	186.04	20.16	0.882

[a] Calculated σ_{iso} values are given as chemical shieldings, and therefore, large values correspond to upfield shifts; signs for $\Delta\sigma$ become opposite to those for the corresponding experimental values

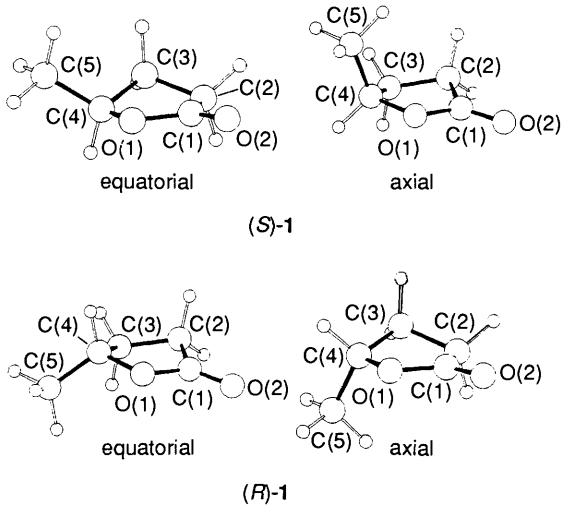

Fig. 5 The equatorial and axial conformers of (*S*)-(−)-γ-valerolactone [(*S*)-**1**] and (*R*)-(−)-γ-valerolactone [(*R*)-**1**] obtained by MM2 molecular mechanics calculations

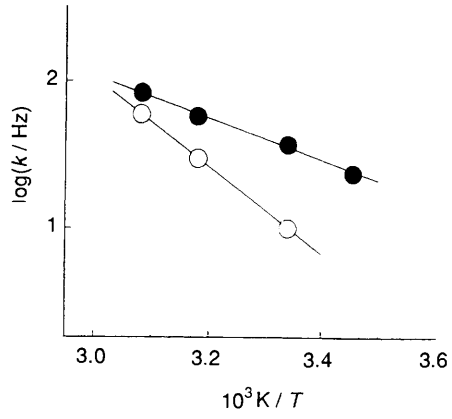

Fig. 6 Temperature dependence of the rate for the reorientation among the octahedral sites for γ-valerolactone (**1**) in the cholic acid/[5-^{13}C]γ-valerolactone inclusion compound (**IV**). Filled and open circles stand for the (*S*)-(−)- and (*R*)-(+)-γ-valerolactone [(*S*)-**1** and (*R*)-**1**], respectively. Solid lines through the data points are the best-fit lines.

The simulation of the powder pattern observed for the C-4 carbon at −23.7 °C gave the $\Delta\sigma$ and η values of −42.2 ppm and 0.64, respectively. Comparison of these values with the ones calculated in Table 2, supports the equatorial conformation of (*S*)-**1** in CAIC. The simulation of the powder pattern obtained for the C-5 carbon at 26.3 °C yielded the $\Delta\sigma$ and η values of −19.1 ppm and 0.00, respectively. These values are essentially identical with those obtained for (*S*)-**1** in **IV** at low temperatures, also supporting the equatorial conformation of (*S*)-**1**.

Molecular Motions of the Enantiomers.—In this section, we have obtained information on the molecular motion of the enantiomers in the CA channels by analysing the temperature-dependent ^{13}C chemical-shift powder patterns of the C-5 carbons for (*S*)-**1** and (*R*)-**1** in **IV**, which are shown in Figs. 3 and 4, respectively. The powder patterns for (*S*)-**1** have a prominent feature, a peak existing at the isotropic resonance position and becoming stronger as temperature increases. This is an indication of the presence of an overall reorientation among a finite number of isotropically located sites as already known.[11,12] We adopted the octahedral or the tetrahedral jump[11] as a molecular motion model for the calculation of the powder patterns. The patterns calculated by the Abragam–Spiess' method showed notable enhancement of the downfield edge and concurrent decrease of intensity in the region between the downfield edge and the isotropic resonance position compared with the observed patterns. The increase of the Gaussian broadening for the calculated patterns is effective for smoothing the downfield edge, but it makes the peak at the isotropic resonance position and the upfield edge merge together. We found that addition[13] of rotational diffusion to the reorientation to a small extent yields better agreement with the experimental spectra. No prominent spectral features were observed for (*R*)-**1** as shown in Fig. 4. We therefore attempted to simulate the variable-temperature spectra by assuming not only the above composite motion model but also other motion models,[12,17] and found that the former model is the most appropriate.

The spectra thus simulated are shown in Figs. 3(*b*) and 4(*b*) for (*S*)-**1** and (*R*)-**1**, respectively, with the rates of the reorientations. The rates of the rotational diffusion are relatively small [1.3–2.3 Hz for (*S*)-**1** and 3.0–4.5 Hz for (*R*)-**1**]. The agreement with the experimental spectra is good in both models with almost the same rates of the reorientation. We therefore cannot state which model is more pertinent; moreover, to be exact, neither octahedral nor tetrahedral reorientation is realistic, because both of the enantiomers and the CA channels are asymmetric. The important point is that the enantiomers reorient among a finite number of nearly isotropically distributed sites.

As mentioned in the previous section, the powder pattern observed for the C-5 carbon of (*S*)-**1** in **III** at 26.3 °C is similar to that observed in **IV** at low temperatures. This result indicates that the molecular motion of (*S*)-**1** in **III** is slower than that in **IV**; in other words, (*S*)-**1** in the CA channels becomes more mobile when (*R*)-**1** is also enclathrated in the CA channels. It, moreover, provides additional evidence that both enantiomers microscopically coexist in the CAIC crystal.

From the Arrhenius plot of the rates of the octahedral jump [the upper values written in Figs. 3(*b*) and 4(*b*)] against reciprocal temperatures shown in Fig. 6, the barriers to reorientation can be evaluated to be 6.5 ± 0.3 and 13.8 ± 0.1

kcal mol^{-1} with the pre-exponential factors of (2.0 ± 1.0) × 10^6 and (1.2 ± 0.2) × 10^{11} s^{-1} for (*S*)-**1** and (*R*)-**1**, respectively.* Thus, (*S*)-**1** undergoes the reorientational motion more rapidly than (*R*)-**1** in CAIC.

When the NMR spectrum for **IV** was measured at 61.3 °C, neither the C-5 signal of (*S*)-**1** nor that of (*R*)-**1** was observed with CPMAS (the cross-polarization time up to 10 ms), but a very sharp singlet was detected by MAS at the average position (21.5 ppm) of the C-5 signals of (*S*)-**1** and (*R*)-**1** in CAIC. This indicates that at this temperature both enantiomers are rapidly and isotropically rotating with concurrent rapid exchange between the equatorial and the axial conformations, suggesting the presence of a phase transition between 51.3 °C and 61.3 °C.

Chiral Discrimination of the Enantiomers.—Since the inclusion process of (*S*)-**1** and (*R*)-**1** into the CA channels can be regarded as a competitive reaction, the relative accommodation factor (RAF) for the selectivity of (*S*)-**1** to (*R*)-**1** can be written according to the definition by Goldup and Smith[18] as eqn. (1), where [CA/(*S*)-**1**] and [CA/(*R*)-**1**] are the weights of

$$\mathrm{RAF} = \{[\mathrm{CA}/(S)\text{-}\mathbf{1}]/[\mathrm{CA}/(R)\text{-}\mathbf{1}]\}/\{[(S)\text{-}\mathbf{1}]/[(R)\text{-}\mathbf{1}]\} \quad (1)$$

the CA-channel sites enclathrating (*S*)-**1** and (*R*)-**1**, respectively, in CAIC, and [(*S*)-**1**] and [(*R*)-**1**] their respective weights in the mixtures from which clathration occurred. The RAF values for the formation of **I** and **II** can be estimated from the values in Table 1, and are the same within the experimental error, indicating the validity of the assumption for the present inclusion process. The free energy difference given by $-\Delta\Delta G = RT \ln \mathrm{RAF}$ amounts to be 0.4 kcal mol^{-1} at 300 K; the positive value indicates that (*S*)-**1** in CAIC is more stable than (*R*)-**1** in CAIC. Since the energies for (*S*)-**1** and (*R*)-**1** are the same in the liquid state, and the CA channels are common to (*S*)-**1** and (*R*)-**1** in CAIC, the free energy difference should directly relate to that between (*S*)-**1** and (*R*)-**1** in CAIC. One should recall that the enclathrated (*S*)-**1** and (*R*)-**1** molecules were found to be in the equatorial and axial conformations, respectively, and that the equatorial conformer was calculated to be *ca.* 0.5 kcal mol^{-1} more stable than the axial in the isolated state. This value is nearly identical to the free energy difference between (*S*)-**1** and (*R*)-**1** in CAIC, leading to the conclusion that the optical resolution of **1** by the inclusion method using the CA host is mainly ascribed to the energy difference in the conformations of the guest **1** molecules.

It is worthy to note that the shape of the five-membered ring of (*S*)-**1** in the equatorial conformation is very close to that of (*R*)-**1** in the axial one (Fig. 5); it suggests that the shape of the five-membered lactone ring plays an important role for the molecular recognition by the CA channel. In this inclusion compound, (*S*)-**1** is not directly recognized; what are recognized by the CA channels are equatorial (*S*)-**1** and axial (*R*)-**1**. The excess of (*S*)-**1** is only caused by the free energy difference between the two conformers of **1**.

Another important result in the present study is on the molecular motions of the two enantiomers in CAIC. Generally, it is thought that the fit of the selected molecules must be as tight as is compatible with the cavity.[19] In the tri-*o*-thymotide clathrate,[20] the major enantiomer is indeed held essentially rigidly, whereas the minor enantiomer is more mobile. In the case of the guest molecules for which little or no enantiomeric excess was found, both enantiomers have, however, the same degree of rotational freedom in the tri-*o*-thymotide clathrate.[20] In the present study of CAIC, we obtained the result that both enantiomers undergo overall reorientation, and that the major enantiomer reorients more rapidly under the lower potential barrier. This observation shows that the above general understanding is not always valid, and chiral discrimination may occur even under the overall isotropic reorientation of the guest molecules.

* The barriers and the pre-exponential factors for the reorientation among the tetrahedral sites for (*S*)-**1** are estimated to be 6.3 ± 0.4 kcal mol^{-1} and (1.5 ± 0.9) × 10^6, respectively, from the Arrhenius plot, which are very close to the corresponding values for the reorientation among the octahedral sites.

Acknowledgements

We thank Prof. M. Miyata of Gifu University and Prof. K. Miki of Tokyo Institute of Technology for valuable discussion and their kind offer of the crystal-structure data prior to the publication. Thanks are due to Dr. S. Obara of Kyoto University for *ab initio* molecular orbital calculations and to Prof. T. Harada of Kyoto Institute of Technology for his kind suggestion about preparation of [5-^{13}C]γ-valerolactone. This work was supported by a Grant-in-Aid for Scientific Research of the Ministry of Education, Science, and Culture, Japan.

References

1 M. Miyata, M. Shibakami, W. Goonewardena and K. Takemoto, *Chem. Lett.*, 1987, 605; K. Miki, A. Masui, N. Kasai, M. Miyata, M. Shibakami and K. Takemoto, *J. Am. Chem. Soc.*, 1988, **110**, 6594; M. Miyata, M. Shibakami, S. Chirachanchai, K. Takemoto, N. Kasai and K. Miki, *Nature*, 1990, **343**, 446; M. Miyata, K. Sada, S. Hori and K. Miki, *Mol. Cryst. Liq. Cryst.*, 1992, **219**, 71.
2 M. Miyata, M. Shibakami and K. Takemoto, *J. Chem. Soc., Chem. Commun.*, 1988, 655.
3 K. Miki, N. Kasai, M. Shibakami, K. Takemoto and M. Miyata, *J. Chem. Soc., Chem. Commun.*, 1991, 1757.
4 J. Ashida, T. Nakai and T. Terao, *Chem. Phys. Lett.*, 1990, **168**, 523; J. H. Iwamiya, M. F. Davis and G. E. Maciel, *J. Magn. Reson.*, 1990, **88**, 199; F. Imashiro, D. Kuwahara, N. Kitazaki and T. Terao, *Magn. Reson. Chem.*, 1992, **30**, 796.
5 R. Ditchfield, *Mol. Phys.*, 1974, **27**, 789; G. E. McMichael, C. Rohlfing, L. C. Allen and R. Ditchfield, *Chem. Phys.*, 1984, **87**, 9; D. B. Chesnut and C. G. Phung, *J. Chem. Phys.*, 1989, **91**, 6238.
6 C. Cardellicchio, V. Fiandanese, G. Marchese and L. Ronzini, *Tetrahedron Lett.*, 1987, **28**, 2053.
7 K. F. Podraza, *Heterocyclic Chem.*, 1987, **24**, 293.
8 D. Kuwahara, F. Imashiro and T. Terao, *Chem. Phys. Lett.*, 1993, **204**, 533.
9 N. L. Allinger, *J. Am. Chem. Soc.*, 1977, **99**, 8127; N. L. Allinger and Y. H. Yuh, *QCPE Bull.*, 1981, **13**, 395.
10 S. Obara, M. Honda, H. Nakano, F. Sakano, S. Takada, Y. Miyake, K. Sato and T. Nakajima, a library program 202 Y4/KOTO91 at the Data Processing Center of Kyoto University (1991); F. Imashiro, Y. Masuda, M. Honda and S. Obara, *J. Chem. Soc., Perkin Trans. 2*, 1993, 1535.
11 H. W. Spiess, *Chem. Phys.*, 1974, **6**, 217; A. Abragam, *The Principles of Nuclear Magnetism*, Clarendon Press, Oxford, 1961, p. 447.
12 J. H. Freed, G. V. Bruno and C. F. Polnaszek, *J. Phys. Chem.*, 1971, **75**, 3385.
13 S. Alexander, A. Baram and Z. Luz, *Mol. Phys.*, 1974, **27**, 441.
14 W. H. Pirkle, D. L. Sikkenga and M. S. Pavlin, *J. Org. Chem.*, 1977, **42**, 384.
15 R. R. Ernst, G. Bodenhausen and A. Wokaun, *Principles of Nuclear Magnetic Resonance in One and Two Dimensions*, Clarendon Press, Oxford, 1987, p. 534.
16 U. Haeberlen, *Advan. Magn. Reson. Supplement 1*, Academic Press, New York, 1976, p. 9.
17 S. Alexander, Z. Luz, Y. Naor and R. Poupko, *Mol. Phys.*, 1977, **33**, 1119.
18 A. Goldup and G. W. Smith, *Sep. Sci.*, 1971, **6**, 791; K. J. Harrington, *Sep. Sci. Technol.*, 1982–83, **17**, 1443.
19 R. Arad-Yellin, B. S. Green, M. Knossow and G. Tsoucaris, in *Inclusion Compounds*, eds. J. Atwood, D. D. MacNicol and J. E. D. Davies, Academic Press, London, 1984, vol. 3, p. 283.
20 J. A. Ripmeester and N. E. Burlinson, *J. Am. Chem. Soc.*, 1985, **107**, 3713; G. Facey and J. A. Ripmeester, *J. Chem. Soc., Chem. Commun.*, 1990, 1585.

Paper 3/03075J
Received 1*st June* 1993
Accepted 21*st June* 1993